ADVANCED FUNCTIONAL MATERIALS
www.afm-journal.de

Hydrogen Production by Solar Photoreforming of Urban Wastewaters in Thin-Layer Flat Catalytic Panels

*Laura C. Valencia-Valero, Kevin A. Simbaña, Margherita Ruscigno, Marta Giamberini, Monika Hapońska, and Alberto Puga**

The effective simultaneous production of hydrogen and removal of organic pollutants by solar photoreforming of various real urban wastewater effluents using a Pt/TiO_2 photocatalyst is proven. Initial testing in laboratory-scale batch photocatalyst suspensions experiments, under both UV and simulated sunlight, result in photocatalytic H_2 production (along with variable CO_2 amounts) from urban wastewaters; photoreforming efficiency decreases in the following order: influent stream > primary sludge > final sludge. Hydrogen evolution exceeds 1500 µmol g_{cat}^{-1} after 3 h under UV. Further development is undertaken in an outdoors pre-pilot-plant scale flat solar panel reactor having a thin layer of photocatalyst (7 g m^{-2}, thickness: 4–30 µm) exposed to natural sunlight. The proof-of-concept solar photoreforming of an influent urban sewage stream in the flat solar panel proceeds with remarkable activity and stability for almost one month (27 d, irradiation time ≈160 h). Despite operated in late autumn at 41.1 ° North latitude, gas production is sustained and consistently correlated with solar irradiances (600–900 W m^{-2}). Furthermore, wastewater decontamination is proven by sustained decrease in chemical oxygen demand and pH, whereas conductivity tended to increase slightly, most likely owing to the breakdown of complex organic matter.

1. Introduction

Hydrogen has emerged as a crucial component in the quest for more sustainable and cleaner energy systems. Its production via water electrolysis (green hydrogen technologies) is advocated as an efficient strategy to store renewable electricity at high mass density, and in turn, as an opportunity to fostering a global shift away from the dependence on fossil fuels.[1] The prospects of hydrogen for the decarbonization of critical sectors of the economy, such as heavy industry and transportation, makes it a promising option in the fight against climate change and in the transition toward a more sustainable and efficient energy future.[2,3] However, hydrogen production, storage, and efficient distribution faces important challenges. From the perspective of raw materials, green hydrogen requires the consumption of large amounts of high-purity water, and hence, it poses pressure on the accessibility to freshwater resources.

The production of hydrogen by photocatalysis represents an alternative to the more common pathway coupling photovoltaics to electrochemical systems. Photocatalysis may greatly simplify the process, given that it can be directly powered by sunlight.[4] Photocatalytic hydrogen production technologies encompass two primary approaches: water splitting and photoreforming. The former process entails the decomposition of pure water into its elements, effectively generating hydrogen and oxygen, analogously to water electrolysis.[5,6] Conversely, photocatalytic reforming, i.e. photoreforming, comprises redox reactions whereby organic matter present in aqueous streams is anaerobically oxidized with concomitant reductive H_2 evolution. Such processes are less demanding due to the relatively low oxidation potentials involved and the favorable kinetics as compared to those of water splitting.[7–10] Moreover, photoreforming does not require previous purification of water effluents; quite the opposite, mixtures of water and a range of organic substances can be used as substrates while achieving the dual benefit of yielding hydrogen. If applied to wastewaters, photoreforming may have potential as an energy-efficient valorization approach.[7,11–13]

Although wastewater treatment technologies are mature and effective, significant issues remain to be solved in the field. Typical biological treatments lead to the generation of sludge, which can be ultimately digested to recover energy in the form of biogas. Albeit well-established, these processes are complex and sensitive to persistent and/or noxious pollutants.[14,15] For this reason, the development of novel wastewater valorization technologies coupling the degradation of organic matter with energy recovery, while minimizing the generation of sludge, are intensely sought alternatives. Among them, the treatment of wastewater by solar photoreforming is perfectly suited since it allows the production

L. C. Valencia-Valero, K. A. Simbaña, M. Ruscigno, M. Giamberini, M. Hapońska, A. Puga
Chemical Engineering Department
Universitat Rovira i Virgili
Av. Països Catalans 26, Tarragona 43007, Spain
E-mail: alberto.puga@urv.cat

The ORCID identification number(s) for the author(s) of this article can be found under https://doi.org/10.1002/adfm.202502903

DOI: 10.1002/adfm.202502903

of hydrogen in a one-step process directly powered by sunlight irradiation.[10,16,17]

For the implementation of solar wastewater photoreforming, efficient and low-cost photocatalysts capable of harnessing sunlight, typically based on semiconductor materials in combination with appropriate co-catalysts, are often employed.[11,18,19] Titanium dioxide (TiO_2) stands out as a prominent semiconductor due to its reasonable response to solar light and high chemical stability in aqueous environments.[20] In addition, it is abundant, economical, and environmentally friendly.[14,15] In order to boost H_2 production, the use of metal cocatalysts is a widely used strategy.[21] Appropriate metallic species deposited on TiO_2 may impart beneficial catalytic effects, by virtue of the ohmic junction established, which enables durable electron-hole separation, efficient electron migration toward metal nanoparticles and eventual transfer to adsorbed acceptor protic species that results in the formation of H_2. The most effective metal for such processes is platinum, showing a much higher production efficiency than the pristine photocatalyst.[22–25]

Despite favorable laboratory-scale results, mostly obtained from batch reactors with powdered M/TiO_2 (*M*: noble metal) photocatalysts in suspension,[26–30] advances in reactor engineering, scale-up and process intensification are still required to consolidate this emerging and rapidly developing technology.[11,31,32] Development and scale-up has primarily relied on tubular reactors mounted on compound parabolic collectors.[17,33] Several studies on hydrogen production during treatment of aqueous effluents have been conducted, using both wastewaters[34–39] or a range of model solutions.[34,40–42] Although these photoreactors achieve high solar light utilization, they also have disadvantages, such as the need to separate the photocatalyst in suspension from the treated aqueous effluent. To reduce the amount of photocatalyst used and avoid separation, thin-layer flat panel photoreactors, onto which the photocatalyst is immobilized, have been proposed for gas-recovery photocatalytic processes,[43–52] both by reforming or overall water splitting.[45,49,51,53] Their modular design and simple construction are key strengths with regards to scalability and implementation feasibility, as proven by the installation of a 100 m^2 solar plant for photocatalytic water splitting on panel reactors,[51] although application of the technology to non-purified or residual aqueous effluents remains unexplored. In this work, the validity of flat solar panels for the direct valorization of urban —i.e. domestic, municipal— wastewaters by photocatalytic reforming, allowing simultaneous hydrogen recovery and decontamination is proven. After initial screening of effluents from different stages of a municipal wastewater treatment plant, including influent and primary/secondary sludges, the effectiveness of photoreforming has been demonstrated in an outdoors pre-pilot-scale flat panel having a thin layer of Pt/TiO_2 (7 g m^{-2}) for almost one month (27 d) under natural sunlight.

2. Results and Discussion

2.1. Laboratory-Scale Urban Wastewater Photoreforming

2.1.1. Hydrogen Production Efficiency

Details of the synthesis and characterization of the Pt/TiO_2 photocatalyst are described in the Experimental Section and in the additional text accompanying Figures S1–S3, Supporting Information. In short, platinum was loaded by impregnation on anatase-rutile nanocomposite titania and activated by thermal reductive treatment under hydrogen. The photocatalytic activity of Pt/TiO_2 was assessed by quantifying the evolution of gaseous products, chiefly hydrogen and carbon dioxide, by photoreforming of representative urban wastewater samples (*Influent* < *Sludge-1* < *Sludge-2*, see Experimental Section and Supporting Information, mainly physicochemical parameters and chemical analyses in Figures S4–S7 and Table S1, Supporting Information, and H_2 and CO_2 yields by photoreforming under simulated sunlight in Table S2, Supporting Information). Error bars, determined by replicate experiments for *Influent* under simulated sunlight, were remarkably independent of irradiation times in absolute terms (±70 μmol g_{cat}^{-1}, Figure S8, Supporting Information). The amount of transition or heavy metals in the wastewater effluents, that could interfere with and affect the photocatalyst, was negligible (Figure S5, Supporting Information).

Initially, photoreforming was studied for *Sludge-1* under UV irradiation (**Figure 1a**) or simulated sunlight (Figure 1b,c). As first observations to note, hydrogen production was feasible in both scenarios, although gas production rates were markedly different. Lower amounts of carbon dioxide (H_2/CO_2 molar ratio above 3) were also produced steadily. Given that TiO_2 is well-known for its effective absorption of UV photons (<400 nm), the significantly faster generation of H_2 when employing strong UV irradiation from a metal-halide lamp as compared to simulated sunlight can be reasonably rationalized. However, the successful production of hydrogen in both cases was surprising and unexpected given the complex nature of the wastewater employed as the substrate. After 3 h of exposure to UV light, noticeable H_2 production (>1500 μmol g_{cat}^{-1}) was recorded, whereas the analogous result obtained after 24 h under simulated sunlight (≈720 μmol g_{cat}^{-1}) was also significant and particularly interesting in the prospect of applying solar photocatalysis to hydrogen production from challenging wastewater effluents. This underscores that the employed photocatalyst can enable the production of hydrogen from domestic sewage effluents of significant physicochemical complexity and high contents of diverse organic and biological matter.

Next, the study of hydrogen evolution was conducted using wastewater samples from different stages in a municipal sewage treatment plant (see Figure S4, Supporting Information), to assess where the photoreforming technology could be more suited in the context of urban wastewater treatment processes. Wastewater sourced after the physical pretreatment (*Influent*), and hence, with minimal qualitative differences to the sewage influent stream flowing into the plant, led to superior H_2 production rates (1307 μmol g_{cat}^{-1} after 24 h of simulated sunlight irradiation, Figure 1b). Notably, hydrogen started being generated even at initial stages of irradiation (2 h). Conversely, more complex sludge streams resulted in much lower production: hydrogen production started after an initial induction period and increased steadily for *Sludge-1*, but it was almost negligible for *Sludge-2*. In order to prove that hydrogen evolution was due to photoreforming of organic matter in the wastewaters, control experiments were performed (Table S3, Supporting Information). After stirring the Pt/TiO_2 photocatalyst

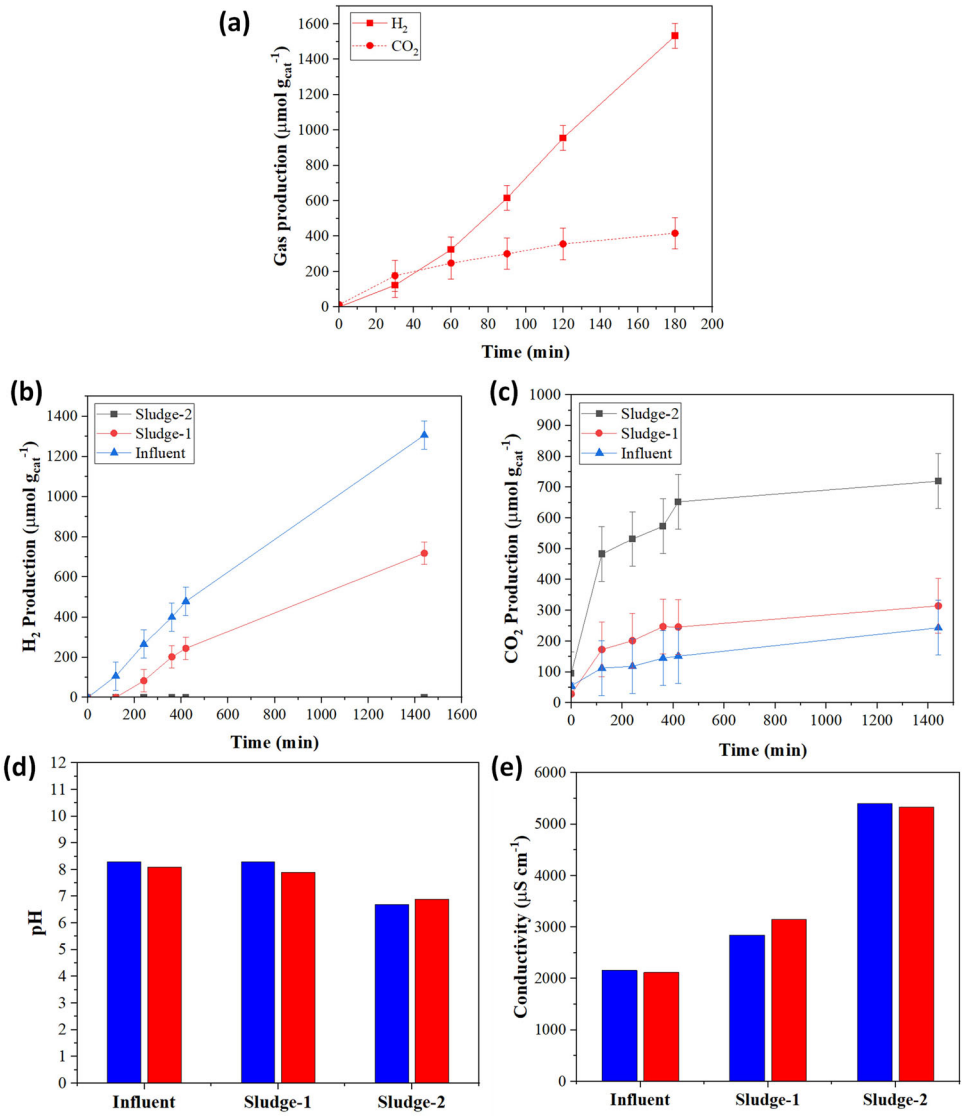

Figure 1. a) Hydrogen and carbon dioxide production by photoreforming of urban wastewaters (Sludge-1, 25 mL). b) Hydrogen and c) carbon dioxide production and evolution of by photoreforming of different urban wastewater effluents under simulated sunlight. Evolution of d) pH and e) conductivity of wastewaters before (blue) and after (red) photoreforming in laboratory-scale experiments for 24 h. Experimental conditions: Suspensions of Pt/TiO_2 (1 g L^{-1}) irradiated with either UV (a, 250 W) or simulated sunlight (b–e, AM1.5G, 100 mW cm^{-2}), under Ar atmosphere.

in *Influent* wastewater in the dark for one day, H_2 production was negligible, and only traces of CO_2 were observed. Prolonged irradiation of *Influent* with simulated sunlight led to a similar outcome. These results demonstrate that hydrogen can be produced by photocatalytic treatment of domestic wastewaters.

The primary difference among these water sources lies in the organic matter content (chemical oxygen demand, i.e. COD, increased in the order: *Influent* < *Sludge-1* < *Sludge-2*, Table S1, Supporting Information). Optical transparency could also be a determining factor, affecting the incidence of photons on the photocatalyst surface. However, electronic spectroscopy shows that absorption between 300 and 400 nm is highest for *Influent* (Figure S7, Supporting Information), and yet, this does not detrimentally affect photocatalytic H_2 production. Light dispersion by suspended solid organic matter in the sludge effluents might also reduce effective photonic absorption by Pt/TiO_2. However, this effect is expected to be minimized under the turbulent stirring mode of the reported batch experiments, whereby the uppermost layers of the reaction media are continuously renovated, and hence, effectively irradiated. Therefore, hydrogen production efficiency by photoreforming is not only affected by the amount of oxidizable organic matter or transparency; the apparently inverted COD-efficiency trend observed strongly suggests that the recalcitrance of wastewaters pollutants, including higher amounts of organic acids (in the form of carboxylates) and phenolic compounds, in addition to biological matter and debris, hinders hydrogen production, especially in the case of *Sludge-2* (Figure S6, Supporting Information). This underscores the complexity of dealing with

real wastewaters and emphasises the need to strategically position the technology within the process. Notwithstanding, the results obtained highlight the viability of utilizing minimally treated urban wastewaters for generating hydrogen by solar photoreforming.

Implementing photoreforming technologies aims not only for hydrogen production but also for reducing the organic load in treated waters. The complete degradation, i.e. mineralization, of organic matter to CO_2 was investigated using gas chromatography (GC) analysis at various irradiation (Figure 1c). The evolution of CO_2 after 24 h of continuous simulated sunlight irradiation for *Influent* was almost 400 µmol g_{cat}^{-1}, ca. one third that of H_2. Conversely, the mineralization extent was relatively low for *Sludge-1* ($H_2/CO_2 \approx 12$). A drastically different behavior was observed for the sludge taken after the secondary treatment (*Sludge-2*), which underwent rapid mineralization during the first hours of irradiation (nearly 500 µmol(CO_2) g_{cat}^{-1} after 1.5 h); notwithstanding slower CO_2 evolution at latter stages, the total amounts evolved were orders of magnitude higher than those of hydrogen. The reason of such drastically different H_2/CO_2 ratios can be in part found in chemical compositions: *Sludge-2* is rich in carboxylates (i.e. acetate, propionate and butyrate, expected by-products of anaerobic digestion, Figure S6, Supporting Information), as detected by ^{1}H magnetic resonance spectroscopy (^{1}H NMR),[54,55] which promptly undergo decarboxylation. The plateau observed in CO_2 evolution, especially for Sludge-2, is related to the presence of such carboxylates. They rapidly undergo decarboxylation at short reaction times and carbon dioxide is released at lower pace after a significant fraction of them is consumed. In contrast, *Sludge-1* is relatively much poorer in those carboxylates, although richer in formate, which readily decomposes into H_2 and CO_2.[8] The laboratory photoreforming experiments presented above clearly indicate that most complex urban wastewater stream, namely the final sludge (COD ≈1.9 10^4 mg L^{-1}, see Table S1, Supporting Information), leads to the formation of CO_2 as the main gas-phase product, and negligible H_2, despite being richest in organic matter. Conversely, less treated —and less complex— sewage and primary sludge effluents (COD values around 10^3 mg L^{-1}) result in notable hydrogen evolution, probably due to the more expedite reforming of simpler organic matter. Due to the characteristics of sludges, containing high amounts of recalcitrant organic matter, their photoreforming is challenging, albeit not impossible.

2.1.2. Wastewater Decontamination Assessment

Studies have shown that photocatalytic hydrogen production can be enhanced by adjusting pH levels to neutral or slightly basic regimes.[56] On the other hand, lower COD levels are preferred for photocatalytic hydrogen production as high COD levels can inhibit the reaction because studies on TiO_2 reveal that a high concentration of contaminants in water saturates the photocatalyst surface and reduces the photonic efficiency, leading to deactivation.[57] Total nitrogen levels can also affect photocatalytic hydrogen production, with higher nitrogen levels leading to lower hydrogen yields.[58] Regarding the wastewaters considered, the influent and primary sludge streams are slightly basic (pH 8.3, Table S1, Supporting Information), whilst the secondary sludge sample has a lower pH value, most likely due to the release of acidic species during the aerobic process and/or during sedimentation in the clarifier, yet close to neutrality (pH 6.7). This was confirmed by ^{1}H NMR, which revealed the presence of substantial amounts of short-chain carboxylates, derived from their parent carboxylic acids, in *Sludge-2* (Figure S6, Supporting Information). After photoreforming under simulated sunlight for 24 h, pH decreased slightly for *Influent* and *Sludge-1*, whereas it increased slightly for *Sludge-2* (see Figure 1d). Such trends can be also rationalized on the basis of chemical composition: photoreforming of less oxidized oxygenated substrates in *Influent* and *Sludge-1* leads to hydrogen evolution and accumulation of acidic by-products in the liquid phase, whereas pH is expected to increase during the predominant release of CO_2 for *Sludge-2*. Interestingly, pH tended to evolve toward neutrality by photoreforming in all cases.

The evolution of conductivity was also studied after photoreforming in laboratory experiments. Initial conductivity was much higher for *Sludge-2*, almost twice as high (5400 µS cm^{-1}) as compared to the less complex streams. Changes in conductivity were small for all wastewaters (see Figure 1e). A non-negligible increase was experienced for *Sludge-1* (2158–3153 µS cm^{-1}), whilst slight declines were observed for *Influent* and *Sludge-2*. By contrast, the outdoors solar experiments performed in the solar panel confirm this decreasing trend in the conductivity of *Influent* upon prolonged sunlight irradiation (see below), probably due to the breakdown of complex organic matter into smaller charged intermediates, e.g. anionic species such as carboxylates. Further work will be devoted to clarifying the underlying phenomena.

2.2. Outdoors Solar Photoreforming in Thin-Layer Flat Panel

2.2.1. Design and Construction of the Panel Reactor

The main motivation of this research was to prove the validity and scalability of panel reactors for the solar photoreforming of urban wastewaters. Immobilization of the photocatalyst in the form of a thin layer exposed to natural sunlight is intended to facilitate its action on contaminants in the aqueous effluent flowing onto it. Based on these premises, the reactor was designed in the form of a rectangular flat panel consisting of a shallow (depth ≈ 15 mm) basin, covered with a technical borosilicate glass (transmittance > 90% above 320 nm), as depicted in **Figure 2a** (see further details in the Supporting Information, including a detailed scheme in Figure S9, Supporting Information). To enable recirculation of the aqueous effluent, the panel had an inlet at the lower part and an outlet at the highest point of the inner basin, which had a roof-like geometry to facilitate gas bubbles to flow out. Mounting of the flat panel reactor was completed with custom sealing gaskets and an enclosing frame.

Deposition of the Pt/TiO_2 photocatalyst was performed by a simple solvent casting method from dispersions in deionized water (see Supporting Information). The thin-layer obtained was adjusted to have a nominal coverage density of ≈7 g m^{-2}. Its thickness was estimated by carrying out an analogous casting procedure as that on the basin of the panel, yet on a glass plate. As observed by scanning electron microscopy (SEM), a continuous thin layer of Pt/TiO_2 (<10 µm) covered the entire surface,

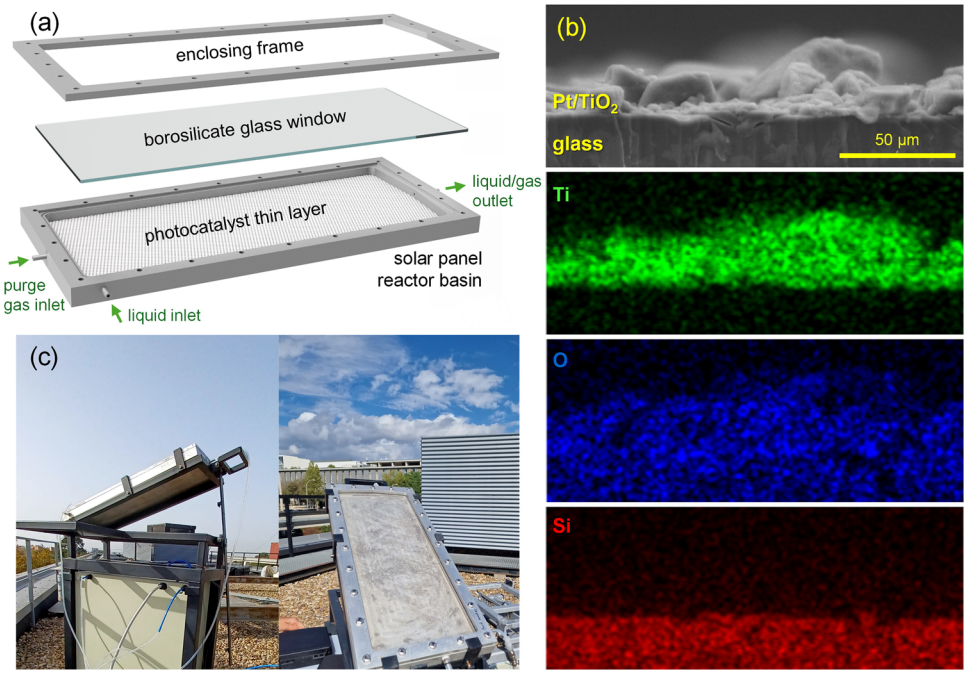

Figure 2. a) Schematic representation of the design of the flat solar panel reactor constructed and employed in this work, consisting of a bottom basin serving as the thin-layer photocatalyst bed and reaction chamber and equipped with inlets for liquid and gas and a combined liquid/gas outlet, a sunlight-transparent borosilicate window, and an enclosing frame, all assembled with rubber gaskets and secured with screws. b) SEM image of the cross-section of a thin layer of Pt/TiO_2 photocatalyst on glass, prepared by an analogous procedure to that used to deposit the thin Pt/TiO_2 layer on the panel reactor basin (top) and derived Ti, O and Si elemental maps obtained by EDS, showing the continuous thin layer of photocatalyst bed on the support. c) Photographs of the solar panel reactor mounted on the tilting scaffold (tilt angle = 30°) in operation under natural sunlight irradiation on the roof of a building in Sescelades Campus at Universitat Rovira i Virgili (coordinates: 41.131633 °N, 1.243671 °E).

whereas some larger protruding grains (≤30 µm) were regularly interspersed; elemental mapping by energy-dispersive X-ray spectroscopy (EDS) clearly confirms the continuous distribution of Pt/TiO_2 (see Figure 2b; Figures S10and S11, Supporting Information). Such a regular thin layer morphology ensures sunlight harnessing across the entire photocatalyst bed surface, whereas its roughness is expected to promote the scattering and reflection of photons impinging at oblique angles when the elevation of the Sun is low —initial or late stages of the daylight period. It is also worth noting that despite using neither binders nor additives, the stability and robustness of the thin layer was satisfactory, that is, no signs of photocatalyst detachment were noticed during months-long set-up and operation.

2.2.2. Testing and Validation of the Panel Under Natural Sunlight

The flat panel reactor operates within a recirculation system whereby the aqueous effluent of interest is pumped from a reservoir tank. A scaffold is used to tilt the panel in order to maximize sunlight irradiation effectiveness and to force any gas bubbles generated by photoreforming to migrate to the upper part of the inner basin (Figure 2c; Figure S12, Supporting Information). The recirculation flow forces the gas to exit the panel basin and leads them back to the reservoir, whereas the gas formed in the headspace there naturally flows through an outlet port to a gas collection tank (see further details in the Supporting Information, a scheme of the reactor system in Figure S13 (Supporting Information) and photographs of the panel in operation in Figure S14, Supporting Information), for volume measurement and sampling.

The system was validated by evaluating the photoreforming activity under natural sunlight using a model aqueous glycerol solution (1% *w*/*v*). The main results of the experiment, namely glycerol concentration evolution and daily gas production volumes, are plotted in Figure S15 (Supporting Information). The effectiveness of organic matter degradation is confirmed by the slow but steady decrease observed in glycerol concentration, i.e. from 11.4 initially to 10.8 g L^{-1} at the end of the experiment (day 16). More importantly, gas evolution took place consistently upon daylight irradiation inside the solar panel in non-cloudy days. The formation and release of bubbles could be even clearly observed by naked eye (as evidenced in video recordings, see Supporting Information). The amounts of gases evolved daily showed a close correlation with maximum solar irradiances and UV indexes, providing evidence about the effective solar photoreforming of aqueous glycerol on the thin layer of photocatalyst in the flat panel reactor.

2.2.3. Photoreforming of Urban Wastewater in Flat Panel Reactor Under Natural Sunlight

After the validation described above using aqueous glycerol, the thin-film solar panel was employed for the photoreforming of a real urban wastewater sample. Among the effluents studied in

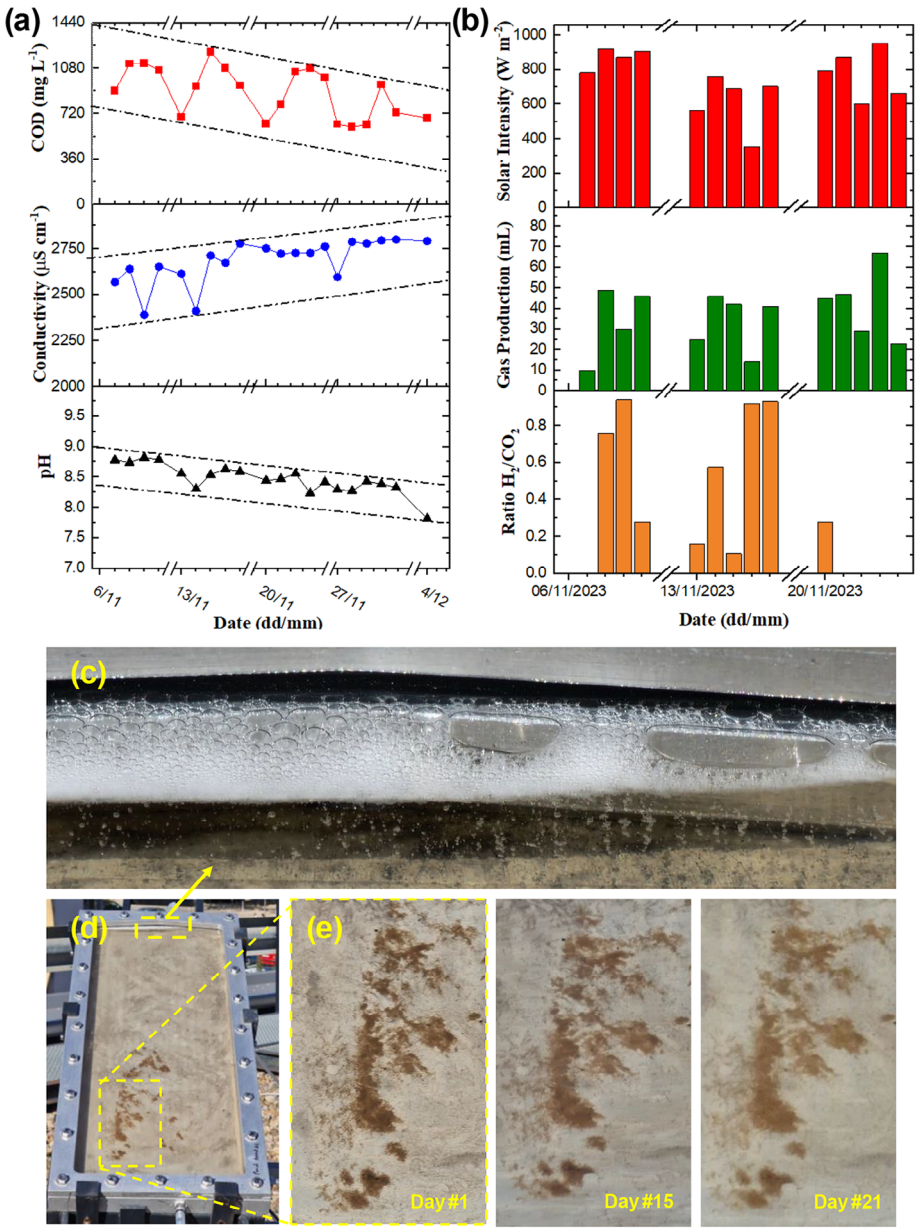

Figure 3. Outdoors photoreforming of *Influent* wastewater in the flat solar panel reactor on a thin Pt/TiO_2 photocatalyst bed layer under natural sunlight irradiation on the roof of a building in Sescelades Campus at Universitat Rovira i Virgili (coordinates: 41.131633 °N, 1.243671 °E), in November/December 2023 (total operation time = 27 d). a) Evolution of physicochemical properties, namely COD, conductivity and pH; dashed-dotted lines are a guide to the eye on the overall evolution trends. b) Correlation of global solar irradiance (top) with daily gas production volumes (middle) and molar H_2/CO_2 ratios (bottom); please note that gas measurements could not be performed after the third week due to dilution after repeated daily purging with Ar to compensate for the volume of withdrawn samples. c) Photograph of the gas produced and accumulated as a foamy layer on the top of the panel cavity, as shown in d) an overall panel photograph, and e) evolution of solids initially present in the wastewater and deposited inside the panel.

laboratory experiments (Section 2.1), *Influent* was selected given the more favorable results obtained with it in terms of photocatalytic hydrogen production. The evolution of various parameters was monitored for nearly four weeks (27 d), including COD, conductivity and pH (**Figure** 3a), to assess decontamination performance, and importantly, gas production volumes and hydrogen/carbon dioxide ratios (Figure 3b), to evaluate the energy-recovery prospects of the photoreforming process. Sunlight irradiances were consistent, yet sub-optimal (600–900 W m^{-2}), given that the experiment was performed in late autumn. Nonetheless, reasonably satisfactory results were obtained, as discussed below. It is worth noting that the photocatalyst did not detach to any substantial extent during the course of the solar experiment, as evidenced by the persistence of the dull grey color of the Pt/TiO_2 bed across the panel. This is remarkable, considering that no binder was used to ensure photocatalyst adhesion.

The results of COD evolution over time in the pre-pilot-scale experiment with *Influent* as the wastewater used in the flat panel

reactor are presented in Figure 3a. Despite some fluctuations, the overall tendency shows a long-term decrease of COD over the course of several weeks. Starting from the initial value of 902 mg L^{-1}, the COD values experience a seesaw trend, to eventually reach 686 mg L^{-1} at the end of the solar experiment (Day 27). Regarding pH, a consistent decrease over time from 8.74 (Day 0) to 7.82 (Day 27) is also apparent (Figure 3a), as expected due to the generation of acidic intermediates during photoreforming of organic substances. This behavior is in agreement with the small-scale batch experiment using *Influent* (see Figure 1d). Conductivity results also show some fluctuations, however an increase over time can be clearly seen (Figure 3a). The conductivity values during the experimental period are in the range between 2390 (Day 3) and 2800 µS cm^{-1} (Day 24). As rationalized above, long-term photoreforming might prompt the breakdown of complex organic matter into smaller fragments, some of them possibly charged (carboxylates or other anionic species) that could result in conductivity increases. Further studies will be performed to better understand these observations.

The evolution of gases by photoreforming of the *Influent* wastewater sample in the flat solar panel reactor under natural sunlight confirmed the favorable results obtained in laboratory experiments. The total amount of gases generated was recorded daily, and samples were analyzed for quantification of H_2 and CO_2 to the best of the system capabilities. Latter measurements (during and after the third week) resulted in the determined amounts of gaseous products below detection limit of the gas chromatograph used, given the repeated headspace gas and liquid sampling over the course of several days, since the withdrawn volumes had to be compensated with the introduction of argon as inert gas.

As observed for the experiment using glycerol, daily gas production volumes were remarkably proportional to the measured maximum irradiance each day around solar noon, except in Day 1, probably due to an induction period prior to full activation of the photocatalyst (Figure 3b). The formation of gas upon sunlight irradiation could be readily observed, and bubbles and foam were slightly accumulated in the upper part of the panel (Figure 3c). Despite the aforementioned difficulties in gaseous product quantification, constant hydrogen production was recorded during the first eight days, with peaks observed on Days 2 and 5. The production of carbon dioxide increased after Day 5, as indicated by the lower H_2/CO_2 ratios (Figure 3b). To identify molecularly simple oxygenated substances and possible intermediate oxidation by-products formed prior to mineralization into carbon dioxide, high-performance liquid chromatography (HPLC) analyses were performed (Table S4, Supporting Information). Acetate, most likely of fermentative origin, was detected, in addition to smaller amounts of formate. The former underwent steady degradation (from ≈34 mg L^{-1} initially) until complete disappearance (Figure S16, Supporting Information). Despite a similarly downward trend, fluctuations in the concentration of formate were observed, a phenomenon that can be related to formic acid production as an intermediate of the photoreforming of oxygenated substances, as demonstrated for carbohydrates in previous research.[59,60] Transient generation of formic, in addition to carbonic or other acids, is a likely cause to the observed progressive pH decrease during the solar photoreforming of *Influent* (Figure 3a), whereas CO_2 evolution due to their decarboxylation is consistent with the trends found in laboratory experiments (Figure 1c).

An additional phenomenon, regarding the observation of solid matter initially present in *Influent* and accidentally deposited inside the panel basin at the start of the experiment, deserves attention. Such solid material, probably organic fibers or biological debris, persisted during the entire length of the solar experiment, but slowly vanished into more diffuse patches (Figure 3d). On the other hand, the anaerobic conditions of the experiment precluded any biological activity. No signs of algae, sludge or biofilms were observed, neither inside the panel, nor inside the rest of the circuit, nor in the reservoir.

Due to the variability in the composition and properties of urban wastewater depending on its origin, making direct comparisons with previous studies is challenging.[12,61] Imizcoz et al. reported low hydrogen production using municipal urban wastewater sample using Au/TiO_2, demonstrating the complexity such effluents, although the reaction times were much shorter than in this work.[26] Similarly, other authors such as Malato et al. reported significant hydrogen production values by photoreforming of urban wastewaters. These and the majority of other related examples describe suspension systems that would require challenging photocatalyst separation steps.[22,25] Other studies worthwhile mentioning report recalcitrant industrial wastewaters.[30,62] Most of other studies in the literature utilizing Pt/TiO_2 rely on model waters,[40,63–65] which do not fully serve as a reference given the complexity of actual urban wastewater. Table S5 (Supporting Information) shows a summary of studies using wastewaters for hydrogen production in solar reactors. From a conceptual point of view, the present work is the first of its kind reporting immobilized thin films of photocatalyst in a flat solar panel reactor for hydrogen production from urban wastewaters, and hence, itrepresents a ground-breaking advancement.

3. Conclusion

The production of hydrogen using the Pt/TiO_2 photocatalyst under UV irradiation and simulated solar radiation with real urban wastewaters was evaluated. The results indicated that influent wastewater exhibited the highest efficiency in hydrogen production, which is a significant finding implicating that this technology could be more effective for certain stages within a wastewater treatment plant, namely for influent streams after minor physical pre-treatment. This is a clear advantage, given that solar photoreforming is feasible as a direct valorization method for urban wastewaters, avoiding the generation of sludge. Although previous studies based on model aqueous substrates suggest that the concentration of organic matter positively influences hydrogen production, an inverse COD-H_2 production relationship is clearly revealed by this study. This indicates that recalcitrance of the organic matter, which is magnified in sludge effluents, plays a crucial role, hindering hydrogen evolution.

Furthermore, flat solar panel reactor with an immobilized thin layer of Pt/TiO_2 as the photocatalyst is valid, robust and effective to treat wastewaters by photoreforming. Both hydrogen production and organic matter degradation took place simultaneously for almost one month (27 d, irradiation time ≈ 160 h) under sub-optimal sunlight irradiances (autumn climate, 600–

900 W m^{-2}). Daily produced gas volumes were directly correlated to average irradiances and UV indexes. Moreover, a progressive decrease in COD and pH, indicating the degradation of organic matter, partly into mildly acidic intermediates, including carboxylic and (ultimately) carbonic acid. In fact, CO_2 generation was observed throughout the solar experiment due to mineralization. Conversely, conductivity tended to increase, probably due to the breakdown of complex organic matter into intermediates including the aforementioned anionic species such as carboxylates. Overall, the results obtained suggest that the developed system represents a significant step toward the valorization of wastewater in treatment plants, allowing not only to produce green hydrogen but also for the degradation of organic matter.

4. Experimental Section

Materials: Aeroxide TiO_2 P25 was obtained as a free sample from Evonik, hydrogen hexachloroplatinate(IV) hydrate (Pt content ≥ 37.5%) was acquired from Sigma–Aldrich, chemical oxygen demand (COD) test tubes (0–15 000 mg L^{-1}) were purchased from Fisher Scientific (Lovibond, Tintometer GmbH, Germany), and glycerol (99.5%) was acquired from Scharlau. All chemicals were used without further purification.

Pt/TiO_2 Photocatalyst Synthesis: The Pt/TiO_2 catalyst was synthesized by a modification of an impregnation-calcination-reduction procedure described by Liu et al.[66] A dispersion of TiO_2 (2.0 g) in deionized water (50 mL) containing H_2PtCl_6 (≈0.8% *w*/*w* Pt/TiO_2 nominal loading ratio) was stirred at room temperature for 2 h and evaporated to dryness. The resulting solid was calcined in air (400 °C, 2 h) and then reduced under H_2/Ar (20:500 mL min^{-1}, 450 °C, 3 h) to yield Pt/TiO_2 as a grey solid.

Wastewater Sourcing and Analyses: Wastewaters were obtained from a municipal wastewater treatment plant (Tarragona, Spain) which operates a typical three-stage process consisting of a physical pre-treatment, primary clarification stage sedimentation tanks, and a secondary aerobic biological treatment followed by final sedimentation tanks (see Figure S4, Supporting Information). Specifically, the wastewater samples used in this work were sourced from largely different stages of the process:

1) *Influent*: taken downstream the physical pre-treatment, having a composition similar to the incoming sewage effluent, but devoid of larger solids (little or no appreciable presence of particles above 0.1 mm).
2) *Sludge-1*: the sedimented fraction drained from the bottom of the primary clarifier, enriched in suspended organic matter or debris.
3) *Sludge-2*: the sedimented fraction drained from the bottom of the secondary clarifier, rich in biological matter that proliferated during the aerobic stage.

Key physicochemical parameters, i.e. pH, conductivity and COD, were determined for as-received wastewater samples; the presence of metals in the samples was ruled out, based on energy-dispersive X-ray analyses (see details in the Supporting Information). Chemical analyses of sludge samples were performed by ^{1}H NMR spectroscopy (see Figure S6, Supporting Information and accompanying discussion).

Laboratory-Scale Photocatalytic Hydrogen Production: In a typical photoreforming experiment, Pt/TiO_2 (25 mg) was dispersed in a sample of the desired wastewater (25 mL) and the resulting suspension sonicated for 10 min, and subsequently transferred to a gas-tight quartz reactor. The reaction mixture was irradiated using a solar simulator equipped with a Xe lamp and an AM1.5G filter (Oriel LCS-100TM) at 100 mW cm^{-1}. Gas samples collected during the irradiation period were analyzed by gas chromatography on a two-channel Agilent 990 Micro GC instrument.

Flat Solar Panel Design and Construction: The solar photocatalytic flat panel reactor used in this work was designed and constructed based on a recent patent application, after scaling up to a larger capacity and a wider irradiation area.[67] It consists of a flat rectangular shallow basin (external dimensions: 30 × 70 cm; effective irradiation area ≈0.14 m^2, see Figure S9, Supporting Information). The Pt/TiO_2 photocatalyst was solvent-casted from an aqueous dispersion on the inner surface of the panel basin. The panel basin was closed with a top borosilicate glass window transparent to nearly the entire solar spectrum, and a closing aluminum frame. The solar reactor system consisted of a closed loop recirculation circuit. A liquid reservoir tank (V = 1 L) was connected to a peristaltic pump that was used to fill the panel. The fluid exiting the panel flows back into the liquid reservoir with its headspace connected to a gas collection tank filled with water (V = 250 mL), which is in turn connected to *i*) a gas sampling port and *ii*) a measuring and pressure compensating cylinder. The system operates at atmospheric pressure and ambient temperature.

Outdoors Photocatalytic Experiments in the Panel Reactor: The panel reactor was then exposed to natural sunlight irradiation on the rooftop of one of the Sescelades campus building of (Universitat Rovira i Virgili, Tarragona, Spain, coordinates: 41.131633 °N, 1.243671 °E). while the liquid was continuously recirculated by means of the peristaltic pump (3 L h^{-1}), and periodic gas and liquid samples were taken for analysis. The liquid reservoir tank was filled with the aqueous effluent to be treated, either aqueous glycerol solution (1% *w*/*v*) or a real wastewater effluent (*Influent*), and the panel reactor was then filled by means of the peristaltic pump. The contents were purged with argon through the liquid sampling valve to ensure anaerobic conditions before the experiments were started. In the case of wastewater photoreforming experiment, the system was filled with *Influent* sample (3 L) and the treatment was continued (start date: November 7th, 2023; end date: December 4th, 2023; total time: 27 d) by maintaining recirculation. Liquid and gaseous samples were analyzed by HPLC and GC, respectively. Daily produced gas volumes were determined at the end of each solar irradiation period (around 16:00). Extended operating details are available in the Supporting Information.

Statistical Analysis: The standard deviation in the amounts of produced gaseous products, chiefly hydrogen, were determined (±70 μmol g_{cat}^{-1}, Figure S8, Supporting Information) by replicate photoreforming experiments for *Influent* under simulated sunlight. The errors observed in pH and conductivity, determined after triplicate measurements for each sample, were ≈±0.01 and ±3 μS cm^{-1}, respectively. Finally, COD replicates could not be performed given that the small volumes of samples were insufficient; the manufacturer of COD reactive tubes suggests relative errors within 0.5%.

Supporting Information

Supporting Information is available from the Wiley Online Library or from the author.

Acknowledgements

This project was funded by the NextGenerationEU programme via the Spanish Research Agency and the European Union (funder: MCIN/AEI/10.13039/501100011033; codes: CPP2021-008619, TED2021-129496B-I00) and by the Generalitat de Catalunya, Agència de Gestió d'Ajuts Universitaris i de Recerca via grant number 2021 SGR 00033. Consortium partners, i.e. FACSA (project coordinator), Enagás and Eurecat, and additional collaborating entities, namely *Consorci Besòs Tordera*, *Transparenta* and the wastewater treatment plant managed by them in Granollers (EDAR Granollers, Barcelona, Spain) are greatly acknowledged for their cooperation in the project. The authors sincerely thank the wastewater treatment plant managing team from Ematsa (Tarragona, Spain) for kindly providing the wastewater samples. L.C.V.-V. thanks Universitat Rovira i Virgili (URV) for a predoctoral contract (Martí i Franquès Program, ref. 2021PMF-PIPF-15). Ernest Arce (Scientific and Technical Resources Service, URV) is gratefully acknowledged for his valuable input into the design of the panel reactor. Dr. Anna Trojanowska is gratefully acknowledged for assitance in performing HPLC analyses.

Conflict of Interest

The authors declare no conflict of interest.

Data Availability Statement

The data that support the findings of this study are available from the corresponding author upon reasonable request.

Keywords

hydrogen, reactor engineering, solar photocatalysis, valorization, wastewaters

Received: January 30, 2025
Revised: May 17, 2025
Published online: October 24, 2025

[1] *Global Hydrogen Review 2023 – Analysis*, **2023**.
[2] Z. Abdin, A. Zafaranloo, A. Rafiee, W. Mérida, W. Lipiński, K. R. Khalilpour, *Renew. Sustain. Energy Rev.* **2020**, *120*, 109620.
[3] *The global energy crisis – World Energy Outlook 2022 – Analysis*, **2022**.
[4] A. Puga, in *Photocatalytic Hydrogen Production for Sustainable Energy*, John Wiley & Sons, Ltd, Hoboken, New Jersey, USA **2023**, pp. 1–18.
[5] S. Chen, T. Takata, K. Domen, *Nat. Rev. Mater.* **2017**, *2*, 1.
[6] A. Kudo, Y. Miseki, *Chem. Soc. Rev.* **2008**, *38*, 253.
[7] Y. Wu, T. Sakurai, T. Adachi, Q. Wang, *Nanoscale* **2023**, *15*, 6521.
[8] A. V. Puga, *Coord. Chem. Rev.* **2016**, *315*, 1.
[9] H. Luo, J. Barrio, N. Sunny, A. Li, L. Steier, N. Shah, I. E. L. Stephens, M.-M. Titirici, *Adv. Energy Mater.* **2021**, *11*, 2101180.
[10] T. H. Jeon, M. S. Koo, H. Kim, W. Choi, *ACS Catal.* **2018**, *8*, 11542.
[11] S. Bhattacharjee, S. Linley, E. Reisner, *Nat. Rev. Chem.* **2024**, *8*, 87.
[12] A. Rioja-Cabanillas, D. Valdesueiro, P. Fernandez-Ibanez, J. Byrne, *J. Phys. Energy* **2020**, *3*, 012006.
[13] S. Y. Toledo-Camacho, S. C Iglesias, in *Photocatalytic Hydrogen Production for Sustainable Energy*, John Wiley & Sons, Ltd, Weinheim, Germany **2023**, pp. 245–273.
[14] J. S. Sravan, L. Matsakas, O. Sarkar, *Bioengineering* **2024**, *11*, 281.
[15] V. Pratap, S. Kumar, B. R. Yadav, *Water Sci. Technol.* **2024**, *90*, 696.
[16] J. Teng, W. Li, Z. Wei, D. Hao, L. Jing, Y. Liu, H. Dai, Y. Zhu, T. Ma, J. Deng, *Angew. Chem., Int. Ed.* **2024**, *63*, 202416039.
[17] A. Ruiz-Aguirre, J. G. Villachica-Llamosas, M. I. Polo-López, A. Cabrera-Reina, G. Colón, J. Peral, S. Malato, *Energy* **2022**, *260*, 125199.
[18] T. Uekert, C. M. Pichler, T. Schubert, E. Reisner, *Nat. Sustain.* **2021**, *4*, 383.
[19] B. Liu, L.-M. Liu, X.-F. Lang, H.-Y. Wang, X. W. (David) Lou, E. S. Aydil, *Energy Environ. Sci.* **2014**, *7*, 2592.
[20] J. Schneider, M. Matsuoka, M. Takeuchi, J. Zhang, Y. Horiuchi, M. Anpo, D. W. Bahnemann, *Chem. Rev.* **2014**, *114*, 9919.
[21] J. Yang, D. Wang, H. Han, C. Li, *Acc. Chem. Res.* **2013**, *46*, 1900.
[22] N. Lakshmanareddy, V. N Rao, K. K. Cheralathan, E. P. Subramaniam, M. V. Shankar, *J. Colloid Interface Sci.* **2019**, *538*, 83.
[23] S. Kim, K. Song, M. Kim, I. Jang, S.-G. Oh, *J. Phys. Chem. Solids* **2013**, *74*, 524.
[24] M. C. Herrera-Beurnio, F. J. López-Tenllado, J. Hidalgo-Carrillo, J. Martín-Gómez, R. Estévez, M. Castillo-Rodríguez, G. de Miguel, F. J. Urbano, A. Marinas, *Catal. Today* **2023**, *413–415*, 113967.
[25] R. M. Navarro, J. Arenales, F. Vaquero, I. D. González, J. L. G. Fierro, *Catal. Today* **2013**, *210*, 33.
[26] M. Imizcoz, A. V. Puga, *Catalysts* **2019**, *9*, 584.
[27] A. Speltini, M. Sturini, F. Maraschi, D. Dondi, A. Serra, A. Profumo, A. Buttafava, A. Albini, *Int. J. Hydrog. Energy* **2014**, *39*, 11433.
[28] A. Speltini, M. Sturini, F. Maraschi, D. Dondi, G. Fisogni, E. Annovazzi, A. Profumo, A. Buttafava, *Int. J. Hydrog. Energy* **2015**, *40*, 4303.
[29] T. Kida, G. Guan, N. Yamada, T. Ma, K. Kimura, A. Yoshida, *Int. J. Hydrog. Energy* **2004**, *29*, 269.
[30] A. Steephen, V. Preethi, B. Annenewmy, R. Parthasarathy, R. P. Reshwanth, M. Sairam, S. Sathish, *Int. J. Hydrog. Energy* **2024**, *52*, 1393.
[31] R. J. Braham, A. T. Harris, *Ind. Eng. Chem. Res.* **2009**, *48*, 8890.
[32] D. Spasiano, R. Marotta, S. Malato, P. Fernandez-Ibañez, I. Di Somma, *Appl. Catal. B Environ.* **2015**, *170–171*, 90.
[33] S. Malato Rodrıǵuez, J. Blanco Gálvez, M. I. Maldonado Rubio, P. Fernández Ibáñez, D. Alarcón Padilla, M. Collares Pereira, J. Farinha Mendes, J. Correia De Oliveira, *Sol. Energy* **2004**, *77*, 513.
[34] K. Villa, X. Domènech, S. Malato, M. I. Maldonado, J. Peral, *Int. J. Hydrog. Energy* **2013**, *38*, 12718.
[35] M. J. Abeledo-Lameiro, A. Hernández Zanoletty, S. Nahim-Granados, M. I. Polo-López, I. Oller, S. Malato, in *Proceedings of the 39th IAHR World Congress*, International Association for Hydro-Environment Engineering and Research (IAHR), Granada, Spain **2022**, pp. 2025–2030.
[36] M. I. Maldonado, A. López-Martín, G. Colón, J. Peral, J. I. Martínez-Costa, S. Malato, *Appl. Catal. B Environ.* **2018**, *229*, 15.
[37] S. Y. Arzate Salgado, R. M. Ramírez Zamora, R. Zanella, J. Peral, S. Malato, M. I. Maldonado, *Int. J. Hydrog. Energy* **2016**, *41*, 11933.
[38] C. Liu, Z. Lei, Y. Yang, Z. Zhang, *Water Res.* **2013**, *47*, 4986.
[39] S. Y. Arzate Salgado, R. M. Ramírez Zamora, R. Zanella, J. Peral, S. Malato, M. I. Maldonado, *Int. J. Hydrog. Energy* **2016**, *41*, 11933.
[40] J. G. Villachica-Llamosas, A. Ruiz-Aguirre, G. Colón, J. Peral, S. Malato, *Int. J. Hydrog. Energy* **2024**, *51*, 1069.
[41] J. G. Villachica-Llamosas, A. Ruiz-Aguirre, G. Colón, J. Peral, S. Malato, *Catal. Today* **2024**, *431*, 114608.
[42] J. G. Villachica-Llamosas, J. Sowik, A. Ruiz-Aguirre, G. Colón, J. Peral, S. Malato, *J. Environ. Chem. Eng.* **2023**, *11*, 111216.
[43] M. Schröder, K. Kailasam, J. Borgmeyer, M. Neumann, A. Thomas, R. Schomäcker, M. Schwarze, *Energy Technol.* **2015**, *3*, 1014.
[44] N. Nalajala, K. N. Salgaonkar, I. Chauhan, S. P. Mekala, C. S. Gopinath, *ACS Appl. Energy Mater.* **2021**, *4*, 13347.
[45] V. R. Battula, G. Mark, A. Tashakory, S. Mondal, M. Volokh, M. Shalom, *ACS Catal.* **2024**, *14*, 11666.
[46] H. Bajpai, I. Chauhan, K. N. Salgaonkar, N. B. Mhamane, C. S. Gopinath, *RSC Sustain.* **2023**, *1*, 481.
[47] A. Xiong, G. Ma, K. Maeda, T. Takata, T. Hisatomi, T. Setoyama, J. Kubota, K. Domen, *Catal. Sci. Technol.* **2014**, *4*, 325.
[48] Q. Wang, T. Hisatomi, Q. Jia, H. Tokudome, M. Zhong, C. Wang, Z. Pan, T. Takata, M. Nakabayashi, N. Shibata, Y. Li, I. D. Sharp, A. Kudo, T. Yamada, K. Domen, *Nat. Mater.* **2016**, *15*, 611.
[49] Y. Goto, T. Hisatomi, Q. Wang, T. Higashi, K. Ishikiriyama, T. Maeda, Y. Sakata, S. Okunaka, H. Tokudome, M. Katayama, S. Akiyama, H. Nishiyama, Y. Inoue, T. Takewaki, T. Setoyama, T. Minegishi, T. Takata, T. Yamada, K. Domen, *Joule* **2018**, *2*, 509.
[50] Q. Wang, Y. Li, T. Hisatomi, M. Nakabayashi, N. Shibata, J. Kubota, K. Domen, *J. Catal.* **2015**, *328*, 308.
[51] H. Nishiyama, T. Yamada, M. Nakabayashi, Y. Maehara, M. Yamaguchi, Y. Kuromiya, Y. Nagatsuma, H. Tokudome, S. Akiyama, T. Watanabe, R. Narushima, S. Okunaka, N. Shibata, T. Takata, T. Hisatomi, K. Domen, *Nature* **2021**, *598*, 304.
[52] C. S. Gopinath, N. Nalajala, *J. Mater. Chem. A* **2021**, *9*, 1353.
[53] M. Schröder, K. Kailasam, J. Borgmeyer, M. Neumann, A. Thomas, R. Schomäcker, M. Schwarze, *Energy Technol.* **2015**, *3*, 1014.
[54] E. G. Alves Filho, L. M. Alexandre E Silva, A. G. Ferreira, *Magn. Reson. Chem.* **2015**, *53*, 648.
[55] S. Navalon, M. Alvaro, H. Garcia, *Environ. Technol.* **2011**, *32*, 295.
[56] M. R. Karimi Estahbanati, N. Mahinpey, M. Feilizadeh, F. Attar, M. C. Iliuta, *Int. J. Hydrog. Energy* **2019**, *44*, 32030.
[57] A. Moses, J. Komandur, D. Maarisetty, P. Mohapatra, S. S. Baral, *Biomass Convers. Biorefinery* **2022**, *14*, 3135.

[58] K. A. Davis, S. Yoo, E. W. Shuler, B. D. Sherman, S. Lee, G. Leem, *Nano Converg* **2021**, *8*, 6.
[59] K. E. Sanwald, T. F. Berto, W. Eisenreich, A. Jentys, O. Y. Gutiérrez, J. A. Lercher, *ACS Catal.* **2017**, *7*, 3236.
[60] L. Lan, H. Daly, R. Sung, F. Tuna, N. Skillen, P. K. J. Robertson, C. Hardacre, X. Fan, *ACS Catal.* **2023**, *13*, 8574.
[61] S. S. Tak, O. Shetye, O. Muley, H. Jaiswal, S. N. Malik, *Hydrog. Energy Technol. Future* **2022**, *47*, 37282.
[62] R. Priya, S. Kanmani, *Environ. Technol.* **2013**, *34*, 2817.
[63] J. J. Velázquez, R. Fernández-González, L. Díaz, E. Pulido Melián, V. D. Rodríguez, P. Núñez, *J. Alloys Compd.* **2017**, *721*, 405.
[64] M. M. Atilano-Camino, A. García-González, D. S. Olivo-Alanís, R. B. García-Reyes, *J. Environ. Chem. Eng.* **2024**, *12*, 112017.
[65] M. Li, Y. Li, S. Peng, G. Lu, S. Li, *Front. Chem. China* **2009**, *4*, 32.
[66] L. Liu, D. M. Meira, R. Arenal, P. Concepcion, A. V. Puga, A. Corma, *ACS Catal.* **2019**, *9*, 10626.
[67] A. Puga, D. Fattoruso, Eur. Pat. 4129931 A1, **2023**.